Online estimation of optimal operating conditions for simulated moving bed chromatographic processes

P. Suvarov[a,c], J.-W. Lee[c], A. Vande Wouwer[a], A. Seidel-Morgenstern[b,c], A. Kienle[b,c,*]

[a]Service d'Automatique, Université de Mons (UMONS), B-7000 Mons Belgium
[b]Otto-von-Guericke-Universität, Universitätsplatz 2, D-39106 Magdeburg, Germany
[c]Max-Planck-Institut für Dynamik komplexer technischer Systeme, Sandtorstrasse 1, D-39106 Magdeburg, Germany

Abstract

A new approach for determining optimal operating conditions for simulated moving bed chromatographic processes is presented. The method is based on recursive online estimation and requires only rough initial estimates. It is based on a simple foot point model of the moving concentration fronts and an online measurement of the corresponding retention times in the different zones of the plant. A mathematical representation of the sdsorption isotherms is not required. The method is validated experimentally for the separation of bicalutamide enantiomers.

Keywords: Chromatography, Simulated Moving Bed, Enantiomers, Triangle Theory, Parameter Estimation

*Corresponding author
Email address: achim.kienle@ovgu.de (A. Kienle)

1. Introduction

Simulated moving bed (SMB) processes represent a powerful technology for continuous chromatographic separations [1]. Besides continuous operation, main advantage compared to batch chromatography is increased productivity. For a detailed discussion for chiral separations the reader is referred to [2, 3].

A typical SMB plant for a binary separation problem to be considered in this paper is illustrated in Fig. 1 together with some characteristic concentration profiles. The plant consists of four columns representing the four zones of a binary separation process. Zone 1 (column 1 in Fig. 1) serves for the regeneration of the solid phase, while zone 4 (column 4 in Fig. 1) serves for the regeneration of the solvent. Separation between components A and B is taking place in zones 2 and 3 (column 2 and 3 in Fig. 1). The stronger adsorbed component (component 'B' in Fig. 1) is collected at the extract while the weaker adsorbed component is obtained at the raffinate. The concentration profiles are moving in the direction of the fluid flow. Countercurrent movement of the solid phase can be achieved by cyclic switching of the in- and outlet ports in the direction of the fluid flow or by column switching in the opposite direction as indicated in Fig. 1.

The performance of the process depends crucially on the operating conditions, which are the flow rate ratios in the four different zones usually termed as m-values (see e.g. [4]). These can be adjusted by the external flow rates indicated by the pumps in Fig. 1 and the switching time.

Usually, the operating conditions of SMB plants are determined *offline* from adsorption isotherms using so-called triangle theory (see e.g. [4]). In

this theory, the operating conditions for total separation represent a triangle in the parameter plane of the flow rate ratios in zones 2 and 3 as illustrated in Fig. 2. Optimal operation with maximum productivity and minimum desorbent requirement is achieved at the vertex of the triangle [5] at point P in Fig. 2. The method is based on an analytic solution of an idealized model assuming isothermal operation, thermodynamic equilibrium, negligible dispersion, and constant flow rates in the different sections of the plant. Due to the analytical approach it is restricted to certain types of isotherms including Langmuir, modified Langmuir and Bi-Langmuir isotherms among others. The latter is often used to describe enantiomers also considered in this paper. In the case of Bi-Langmuir isotherms, the design is not explicit anymore leading to different shortcuts as discussed in [6, 7]. An extension of this design approach to processes with Langmuir isotherms and reduced purities was discussed in [8].

The key information required in all of these approaches is the knowledge of the adsorption isotherms, which are usually determined a priori from single column experiments. However, adsorption characteristics may change with time due to unavoidable aging of the solid phase. In addition, the separation is influenced by (often not precisely known) dead volumes introduced by the tubes and fittings [9] [9, 10]. In the present paper we therefore propose a new approach for the (re)adjustment of the optimal operating conditions for total separation corresponding to the vertex of the triangle in Fig. 2, without explicit knowledge of the triangle. The method is based on recursive *online* estimation and requires only rough initial estimates. It relies on measurement of retention times in the different zones of the SMB plant and uses

a simple foot point model to describe the movement of the concentration fronts. Adsorption isotherms are not explicitly required. It therefore applies to any adsorption isotherm, provided total separation is feasible at all. Dead volumes are automatically taken into account.

The method was first proposed by Fütterer [11] and later elaborated by Suvarov [12, 13]. In these papers, focus was on cycle to cycle adaptive control of SMB plants. The parameter estimator was used as a component of the control concept and not considered independently. In the present paper, focus is on the estimator. It is validated experimentally and its relation to triangle theory is discussed. Preliminary results have been presented in the PhD Thesis of Suvarov [14].

2. Theoretical Approach

The dynamics of the SMB plant is characterized by moving concentration fronts as illustrated in Fig. 1. The online estimator is based on a simple discrete time model of the moving concentration fronts. The front movement is described with the movement of the foot points as shown in Fig. 1. A typical situation of a concentration front traveling between two neighboring zones is illustrated in Fig. 3. A dimensionless retention time τ is introduced, which represents the percentage of the cycle time the foot point is in the left column of Fig. 3. Accordingly, $1 - \tau$ represents the dimensionless retention time in the right column. τ can be measured for example with a UV detector as also illustrated in Fig. 3. For that purpose a certain threshold is introduced as shown in Fig. 1 to compensate for measurement noise.

Using the retention time τ, the distances the foot point is traveling in the

left and the right column can be expressed according to Fig. 3 as

$$\Delta z_l(k) = v_l(k) T_{SW}(k) \tau(k), \tag{1}$$

$$\Delta z_r(k) = v_r(k) T_{SW}(k) (1 - \tau(k)). \tag{2}$$

After switching, the wave is shifted by one column length according to

$$\Delta z_l(k+1) = L - \Delta z_r(k) \tag{3}$$

as illustrated in Fig. 3. The characteristic velocities of the foot points v_i can be calculated from equilibrium theory using the method of characteristics [15]. It is proportional to the volumetric flow rate Q_i of the fluid phase and some parameter Θ which depends on the properties of the adsorbent [15]

$$v_i(k) = Q_i(k) L / \Theta, \qquad i = l, r \tag{4}$$

Substitution of Eqs. (1, 2, 4) into Eq. (3) gives a one step ahead predictor for the retention time in Fig. 3 according to

$$\hat{\tau}(k+1) = \frac{\Theta - Q_r(k) T_{SW}(k) (1 - \tau_i(k))}{Q_l(k+1) T_{SW}(k+1)} \tag{5}$$

In the following it is assumed that the two regeneration fronts on the extract side of Fig. 1 are moving back and forth between zone 1 and 2 and the two adsorption fronts on the raffinate side of Fig. 1 are moving back and forth between zones 3 and 4. The back shifting is due the cyclic repositioning of the in- and outlets.

Let us define τ_1 as the retention time of the first front in Fig. 1 in zone 1 of the SMB plant, τ_2 the retention time of the second front in Fig. 1 in zone 2

of the SMB plant and so on for τ_3 and τ_4. Then, in analogy to the derivation above the following expressions for the retention times τ_i are obtained

$$\hat{\tau}_i(k+1) = \frac{\Theta_i - Q_r(k)T_{SW}(k)(1-\tau_i(k))}{Q_l(k+1)T_{SW}(k+1)}, \qquad i = 1, 3, \tag{6}$$

$$\hat{\tau}_i(k+1) = 1 - \frac{\Theta_i - Q_r(k)T_{SW}(k)(\tau_i(k))}{Q_l(k+1)T_{SW}(k+1)}, \qquad i = 2, 4.. \tag{7}$$

Therein, Q_l and Q_r are the flow rates in zone 1 and 2 for τ_1 and τ_2 and the flow rates in zone 3 and 4 for τ_3 and τ_4.

Using these expressions, the Θ parameters can be estimated online by comparison of predicted and measured retention times $\hat{\tau}_i$, and τ_i as illustrated in Fig. 4 for Θ_1. For that purpose the following recursive estimator control law is applied

$$\hat{\Theta}_i(k+1) = \hat{\Theta}_i(k) + (1 - K_\theta)\Delta\Theta_i(k), \tag{8}$$

with

$$\Delta\Theta_i(k) = \Theta_i - \hat{\Theta}_i = Q_i(k)T_{SW}(k)(\tau_i(k) - \hat{\tau}_i(k)). \tag{9}$$

and the gain K_Θ. The absolute value of K_Θ has to be smaller than one for stable operation. The recursion converges for $\hat{\tau}_i(k) = \tau_i(k)$ to $\hat{\Theta}_i = \Theta_i$.

Finally, the significance of the Θ parameters and their relation to the well known triangle theory (see e.g. [4]) is discussed. At cyclic steady state, the flow rates, the switching times, and the retention times are constant, e.g.

$$\tau_i(k+1) = \tau_i(k) = \tau_i. \tag{10}$$

Further, for total separation at point P with maximum feed and minimum solvent consumption in Fig. 2 all retention times are equal to one

$$\tau_i = 1, \tag{11}$$

i.e. each front is moving back and forth in its respective zone. This can be explained in the following way:

$\tau_1 = 1$ follows from total regeneration of the solid phase in zone 1 with minimum solvent consumption. Total regeneration in zone 1 implies no breakthrough of component B to zone 4 in Fig. 1. Minimum solvent feed is achieved if the foot point of the corresponding concentration front is located at the very left of zone 1 at the beginning of each cycle. Higher solvent feeds would lead to a foot point position in the middle of zone 1 at the beginning of the cycle and consequently to a foot point position in the middle of zone 2 at the end of the cycle.

$\tau_2 = 1$ follows from the condition of a pure extract with minimum solvent consumption. Pure extract implies no breakthrough of component A to zone 1 in Fig. 1. Minimum solvent feed is achieved if the foot point of the corresponding concentration front is located at the very left of zone 2 at the beginning of the cycle.

$\tau_3 = 1$ follows from the condition of a pure raffinate with maximum feed rate. Pure raffinate implies no breakthrough of component B to zone 4 in Fig. 1. Maximum feed rate is achieved if the foot point of the corresponding concentration front is located at the very right of zone 3 at the end of the cycle. Lower feed rates would lead to a foot point position in the

middle of zone 3 at the end of the cycle and after switching to a foot point position in zone 2 at the beginning of the new cycle.

$\tau_4 = 1$ follows from total regeneration of the solvent in zone 4 with maximum feed rate. Total regeneration in zone 4 implies no breakthrough of component A to zone 1 in Fig. 1. Maximum feed rate is achieved if the foot point of the corresponding concentration front is located at the very right of zone 4 at the end of the cycle. Note, that this is not fully achieved in Fig. 1, because the operating conditions used in this figure were not optimized.

Substitution of Eqs. (10) and (11) into Eqs. (6) and (7) yields

$$\Theta_i = Q_i T_{SW}. \tag{12}$$

That means that, the Θ parameters are directly related to the optimal operating conditions of the triangle theory at point P in Fig. 2.

In the triangle theory, operating conditions are given in terms of m-values which represent the ratio of the net transport in the fluid phase and the net transport of the solid phase due to switching. For SMB processes these m-values are defined as [4]

$$m_i = \frac{Q_i T_{SW} - V\epsilon}{V(1-\epsilon)}. \tag{13}$$

In view of Eq. (12) we finally find the following relation between the m-values and the Θ parameters

$$\Theta_i = V\left(m_i(1-\epsilon) + \epsilon\right). \tag{14}$$

3. Experimental Validation

3.1. Methods and materials

The SMB unit consists of one 48-port valve tower (C912, Knauer GmbH, Germany), four pumps (K-1800, Knauer GmbH, Germany), and two UV detectors (K-2501, Knauer GmbH, Germany). Two 250 ml of glass bottles were connected at each product stream outlets of the SMB unit with 6-port 2-position valve (Knauer GmbH, Germany). An HTS/PAL autosampler (CTC analytics AG, Swiss) collects samples from two product stream bottles and injects collected samples to an analytical HPLC unit (Knauer GmbH, Germany). Four preparative columns (2.5 x 14.7 cm, $\epsilon = 0.78$) packed with ChiralPak IA (20 μm, Daicel Chemical Industries Ltd., Japan) were connected in the SMB unit with one column per zone configuration. An analytical column (ChiralPak IA, 3 μm, 0.46 x 15 cm, Daicel Chemical Industries Ltd., Japan) was used to analyze the feed mixture and collected product samples during the SMB operation. The pump flow-rates and the valve motions were controlled and the detector signals were acquired by an interface software developed with LabVIEW (National Instruments Inc., USA, Ver. 11).

In the analytical HPLC unit, HPLC grade methanol (VWR GmbH, Germany) was used as the mobile phase. The flow-rate was 2.0 ml/min, the injection volume was 5.0 μl, and the column temperature was fixed to 40 C. The analysis time for two samples was 140 seconds. During one port switching interval, one bottle is used to collect the SMB outlet effluent with constant stirring condition (200 rpm), and the autosampler collects the sample from the other bottle that was used to collect the SMB outlet effluent in previous port switching interval. After collecting samples, the bottle is

flushed with nitrogen gas (1.5 bar) to remove collected effluent, and then the empty bottle is used to collect SMB outlet effluent in next port switching interval.

The feed mixture, racemic bicalutamide (AstraZeneca AB, Sweden) was dissolved in ACS grade methanol (Merck, Germany). The same grade of methanol was used as the mobile phase. The collected UV detector signal from the analytical HPLC unit (254 nm) was calibrated to convert the peak area to the concentration (up to 16.6 g/L of racemic mixture), and the UV detector signals from the outlet stream of the SMB unit (both 300 nm) were collected for the state estimator and the controllers.

3.2. Results

The first experimental results for the parameter estimator validation are illustrated in Fig. 5 in terms of product purities and estimated as well as applied m-values. The experiment is started with fully regenerated columns. Initial operating parameters were calculated from triangle theory with some safety margins assuming linear isotherms. The full blown nonlinear isotherm was not known. The initially calculated m-values are given in Table 1. After startup during the first ten cycles corresponding to period 1 in Fig. 5 a steady state with relatively low raffinate purity of about 70 % is attained. From this it is concluded that linear isotherms do not apply due to the relatively high feed concentration of 10 g/l of racemic mixture, which is obviously in the nonlinear range of the adsorption isotherms. In parallel, the estimator converges to a new set of parameters which are expected to deliver a high product purity of both products under operating conditions which are very close to the optimal ones. Parameter estimates are shown in the lower

diagram of Fig. 5 in terms of m-values. From this figure it is concluded that m_2 is already close to the estimated optimal value, which is reflected in the high product purity of the extract, whereas m_3 needs improvement to achieve also high raffinate purity. Deviations of m_1 and m_4 from the estimated values are relatively high due to the very conservative initialization.

Afterwards, during the second period in Fig. 5. PI controllers are activated to ensure total regeneration in zones I and IV. Controllers have been described in detail in [13]. For robustness, reference values for τ_1 and τ_4 of 0.5 are given instead of the theoretical values of 1. Consequently, m_1 and m_4 are adjusted automatically by the controller to some new values which deviate from the estimated ones but ensure total regeneration under varying operating conditions in the remainder.

Subsequently, in the third and fourth period of Fig. 5, m_2, and in particular, m_3 is readjusted in two steps to the estimated value. The resulting steady state shows indeed a high purity of both product flows, which validates the parameter estimator. Final operating conditions are also shown in Table 1.

Finally, the fifth and sixth steps are used to determine the maximum throughput of the SMB unit without violating the internal flow rate constraint of 100 ml/min and the maximum operating pressure of the plant. For that the switching time is decreased from initially 178 s to 89 s in period five and 70 s in period 6.

The experiment has been repeated in a similar way for periods 1 to 4 more than one year later. Periods 5 and 6 have been omitted. Results are shown in Fig. 6. Starting values are the same as in the first experiment.

Final values of this second experiment are also shown in Tab. 1. Clearly, the final values of the second experiment differ from the first experiment which is due to column aging. We conjecture that these different operating conditions are due to some aging of the solid phase, since in between many other experiments were run on this plant. Further, the temporal evolution of the measurement signals in Figs. 5 and 6 also differs qualitatively. This is due to the fact that sensor and pump location have been interchanged between the experiments. In Fig. 5 sensors are located in the direction of the fluid flow before the pumps. In Fig. 6 it is the other way round. Again, raffinate purity is rather low in the beginning compared to the extract purity which is mainly due wrong initial guess in m_3. Consequently, after readjustment in two steps both products are obtained with high purity.

Right afterwards, a third experiment was performed, illustrated in Fig. 7. Initial operating conditions correspond to the final values of the second experiment due to Table 1. To demonstrate close to optimal operation of this operating points perturbations of m_2 and m_3 were applied. According to the schematic triangle in Fig. 2 one would expect that an increase in m_3 leads to a decrease in raffinate purity whereas an decrease in m_2 leads to a decrease in extract purity for an operating point close to the tip of the triangle. In principle, Both patterns of behavior can be observed in Fig. 7. However, extract purity is much more sensitive to changes in m_2. It is worth noting that the triangle in Fig. 2 is only schematic. The exact triangle was not known since the nonlinear adsorption isotherms were not known. In both cases in Fig. 7 a step change of 5 % was applied to the internal flow rates and then converted to m-values. The experiment clearly shows that

the parameter estimator delivers values close to the optimum.

4. Conclusion

In the present paper a new approach for online estimation of optimal operating conditions for total separation of binary mixtures in SMB plants was presented and validated experimentally. Limitations of the approach arise from the underlying assumptions of the foot point model. Desorption fronts should be located in zones 1 and 2 and adsorption fronts should be located in zones 3 and 4. In particular, total regeneration in zones 1 and 4 is required, which can be achieved automatically with standard PI control as described in [13, 14]. The above requirements can further be met by suitable initial guesses. In the present case, initial guesses for the nonlinear separation were generated from Henry coefficients.

It should be further stressed, that optimality of the operating conditions refers to triangle theory, which assumes negligible mass transfer resistance between fluid and solid phase and negligible axial dispersion in the fluid phase leading to shock waves in zones 3 and 4 for favorable adsorption isotherms. For systems with finite mass transfer resistance and finite axial dispersion the slopes of concentration fronts will be finite giving rise to some deviations from optimality and/or total (i.e. 100 %) separation. However, it was shown in our third experiment that these deviations are relatively small for practical cases, if the columns are efficient enough.

The number of cycles to meet the final specifications is relatively high in Figs. 5 and 6. This however is due to the rather conservative experimental strategy applied in phases 1 to 4 of these experiments, where a lot of time

is given in each phase to settle down to the new conditions. The temporal evolution in these Figures indicates that the number of cycles can be reduced, which, however, was not the objective of this work.

In the present paper the parameter estimator was used for (re)adjustment of the operating conditions. However, it is worth noting that it can also be used for feed-back adaptive cycle to cycle control of product purities as described in [11, 13, 14]. With feed-back control of product purities, unforeseen disturbances can be rejected automatically and the product purities can be adjusted to any reasonable given value. This can be attractive to increase the productivity of the plant for less restrictive purity requirements (see e.g. [8, 16]).

Notation

K_Θ	estimator gain [-]
m	m-values of triangle theory defined in Eq. (13) [-]
Q	flow rate [m^3/s]
T_{SW}	switching time [s]
v	propagation velocity [m/s]
V	column volume [m^3]
z	spatial coordinate [m]

Greek Letters

ϵ	void fraction of the bed [-]
τ	normalized retention time [-]
Θ	parameters defined in Eq. (4) [m^3]

Sub- and Superscripts

i	zone number
k	time step

[1] H. Schmidt-Traub, M. Schulte, and A. Seidel-Morgenstern. *Preparative Chromatography*. Wiley-VCH, Weinheim, 2012.

[2] M. Schulte and J. Strube. Preparative enantioseparation by simulated moving bed chromatography. *J. Chrom. A*, 906:399–416, 2001.

[3] A. Rajendran, G. Paredes, and M. Mazzotti. Simulated moving bed chromatography for the separation of enantiomers. *J. Chrom. A*, 1216:709–738, 2009.

[4] C. Migliorini, M. Mazzotti, and M. Morbidelli. Continuous chromatographic separation through simulated moving beds under linear and nonlinear conditions. *J. Chromatogr. A*, 827:161–173, 1998.

[5] M. Mazzotti, G. Storti, and M. Morbidelli. Optimal operation of simulated moving bed units for nonlinear chromatographic separations. *J. Chrom. A*, 769:3–24, 1997.

[6] C. Migliorini, M. Mazzotti, and M. Morbidelli. Robust design of countercurrent adsorption separation processes: 5. Nonconstant selectivity. *AIChE J.*, 46:1384–1399, 2000.

[7] M. Kaspereit and B. Neupert. Vereinfachte Auslegung der simulierten Gegenstromchromatographie mittels des Hodographenraumes. *Chemie-Ing.-Techn.*, 88:1628–1642, 2016.

[8] M. Kaspereit, A. Seidel-Morgenstern, and A. Kienle. Design of simulated moving bed processes under reduced purity requirements. *J. Chromatogr. A*, 1162:2–13, 2007.

[9] C. Migliorini, M. Mazzotti, and M. Morbidelli. Simulated moving-bed units with extra-column dead volume. *AIChE J.*, 45:1411–1421, 1999.

[10] P. S. Gomes, M. Zabkova, M. Zabka, M. Minceva, and A. E. Rodrigues. Separation of chrial mixtures in real SMB units: The FlexSMB-LSRE®. *AIChE J.*, 56:125–142, 2010.

[11] M. Fütterer. On design and control of simulated moving bed processes, 2010. Ph.D. Thesis, Otto-von-Guericke-Universität Magdeburg.

[12] P. Suvarov, A. Vande Wouwer, A. Kienle, C. Nobre, and G. De Weireld. Cycle to cycle adaptive control of simulated moving bed chromatographic separation processes. *J. Proc. Contr.*, 24:357–367, 2014.

[13] P. Suvarov, A. Vande Wouwer, J. W. Lee, A. Seidel-Morgenstern, and A. Kienle. Control of incomplete separation in simulated moving bed chromatographic processes. In *Proc. 11th IFAC Symposium on Dynamics and Control of Process Systems, including Biosystems*, Trondheim, June 6-8, 2016. IFAC-Papers-Online, Volume 49, Issue 7, p. 153-158.

[14] P. Suvarov. Robust control methods for simulated moving bed chromatographic processes, 2016. Ph.D. Thesis, Otto-von-Guericke-Universität Magdeburg & University of Mons (Cotutelle).

[15] Hyun-Ku Rhee, Rutherford Aris, and Neal R. Amundson. *First-Order Partial Differential Equations: Volume II – Theory and Application of Hyperbolic Systems of Quasilinear Equations*. Prentice Hall, New Jersey, 1989.

[16] M. Kaspereit, S. Swernath, and A. Kienle. Evaluation of competing process concepts for the production of pure enantiomers. *Org. Process Res. Dev.*, 16:353–363, 2012.

List of Tables

	m_1	m_2	m_3	m_4
Experiment 1				
initial operating point	6.50	0.857	2.379	-1.2
final operating point	3.414	0.866	1.442	-0.538
Experiment 2				
initial operating point	6.50	0.857	2.379	-1.4
final operating point	4.26	0.74	1.30	-0.61

Table 1: M values for the initial and final operating points of the experiments.

List of Figures

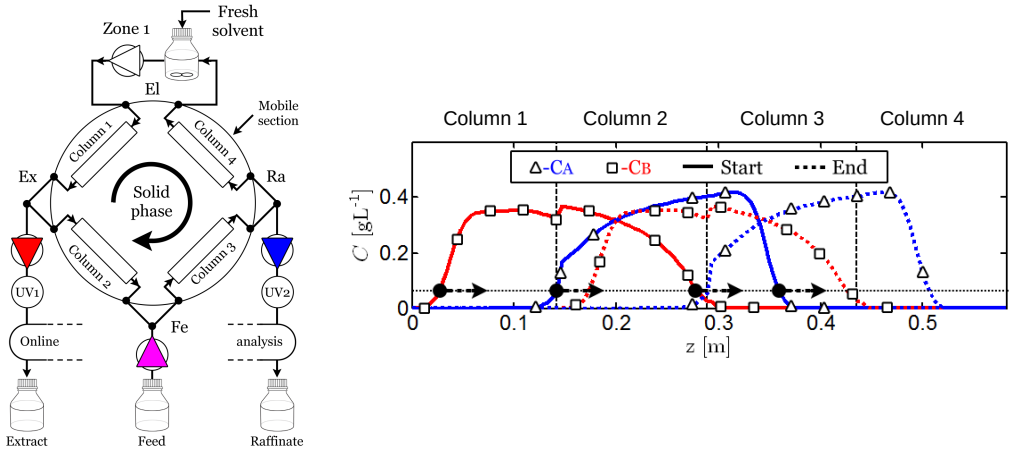

Figure 1: Simulated moving bed chromatographic process. Left: plant configuration, right: temporal evolution of concentration profiles. Figure reproduced from reference [13] with kind permission of IFAC.

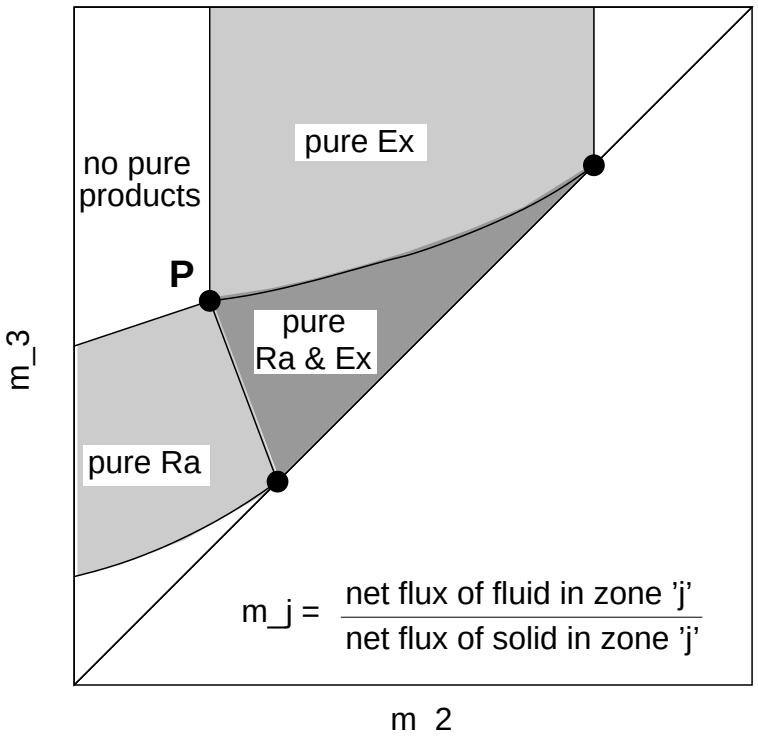

Figure 2: Separation regions in the m_2, m_3 parameter plane according to [4].

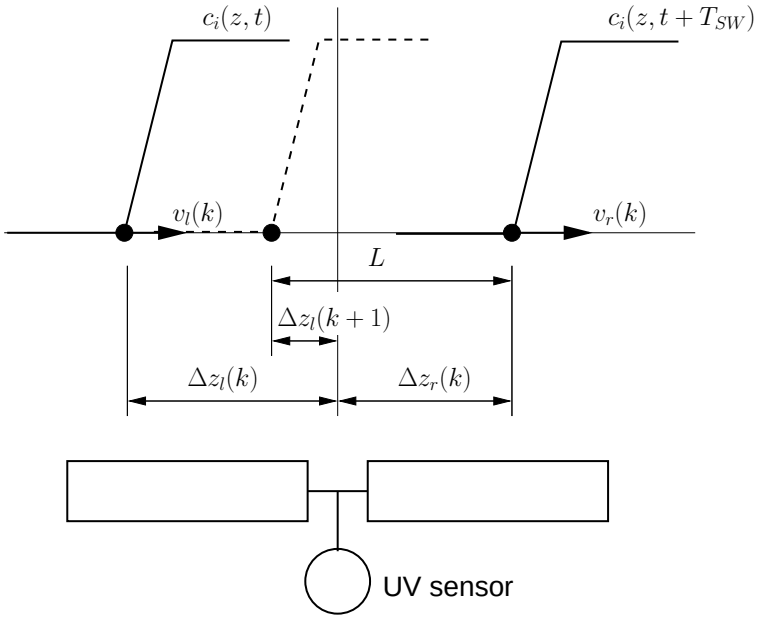

Figure 3: Illustration of the foot point model.

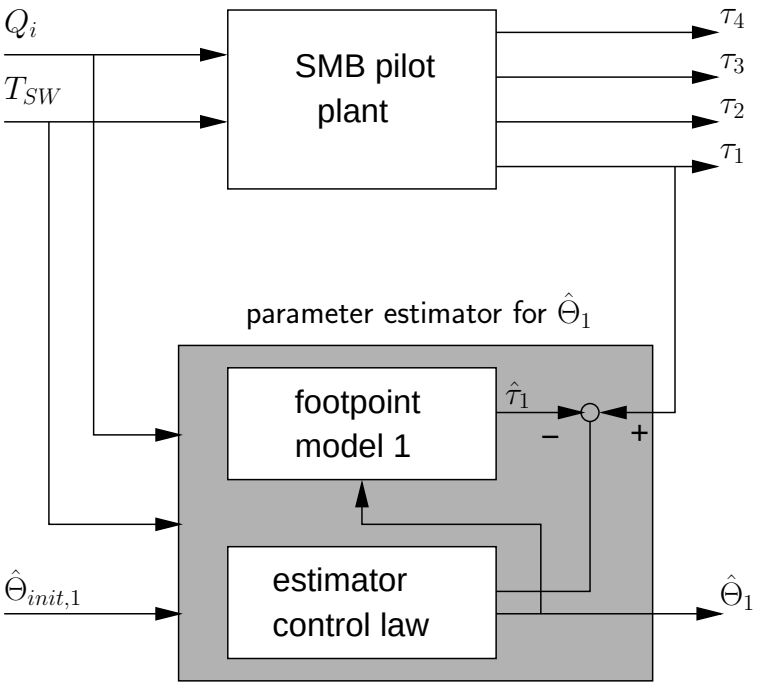

Figure 4: Block diagram of the parameter estimator for Θ_1.

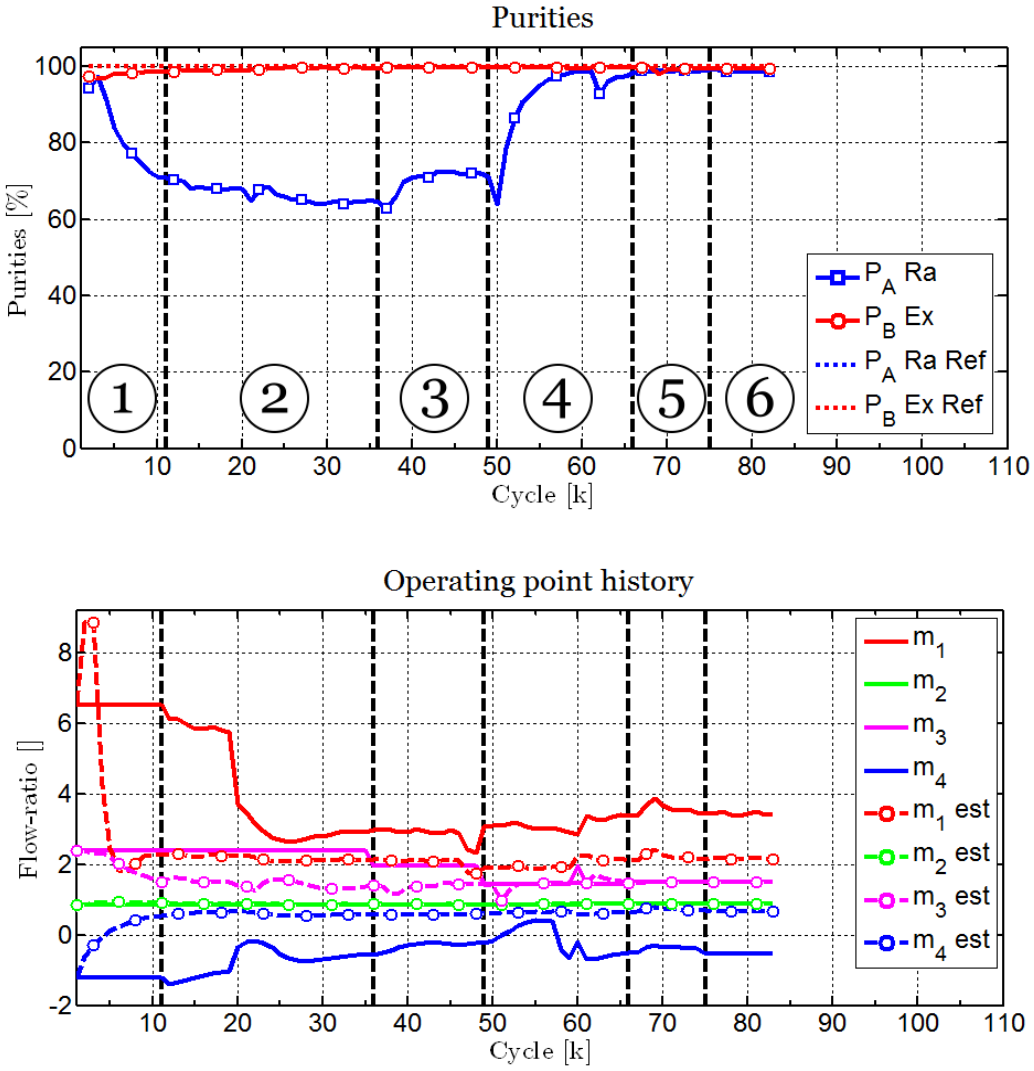

Figure 5: First experimental validation of the parameter estimator. Startup from wrong initial conditions as given in Table 1. Final operating conditions determined by the parameter estimator are also given in Table 1.

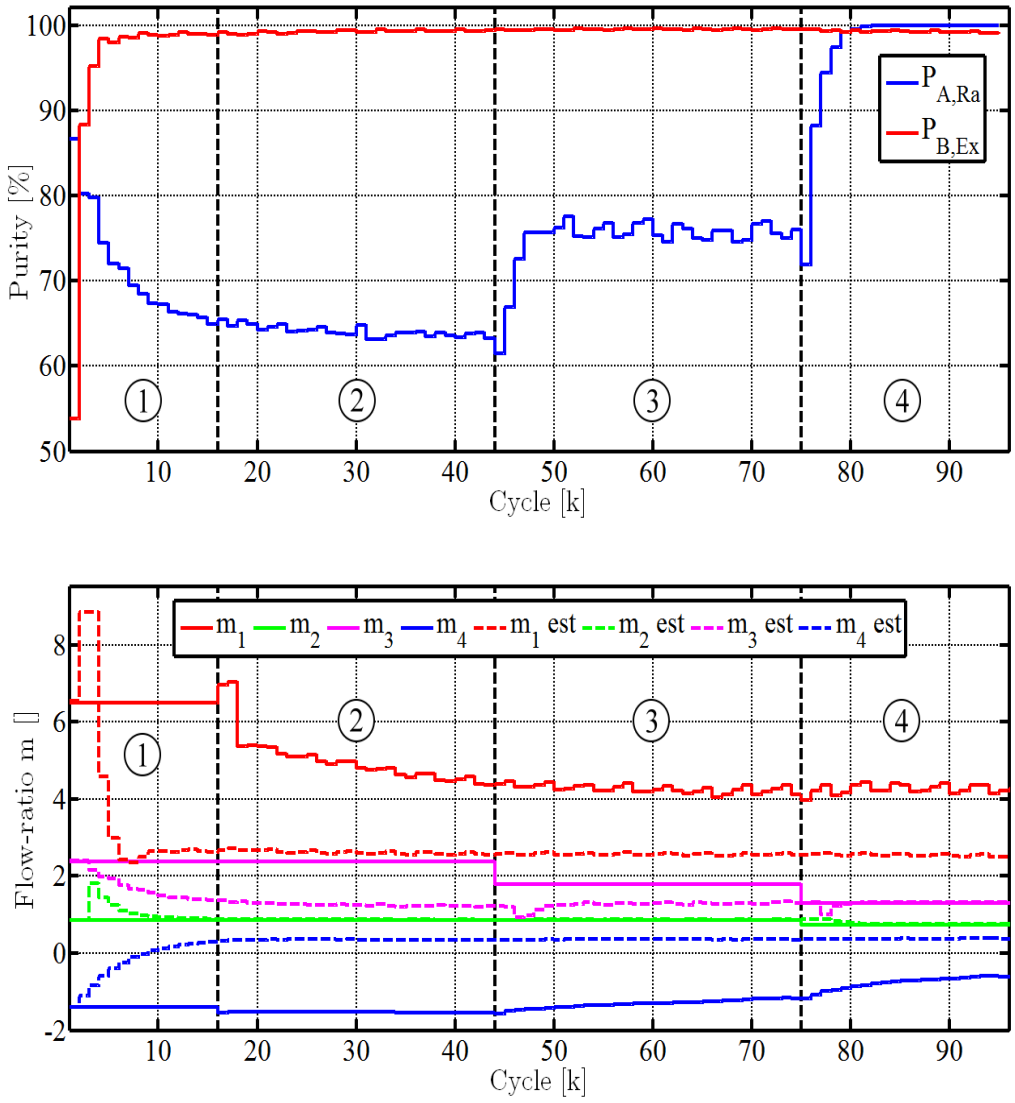

Figure 6: Second experimental validation of the parameter estimator. Startup from wrong initial conditions as given in Table 1. Final operating conditions determined by the parameter estimator are also given in Table 1.

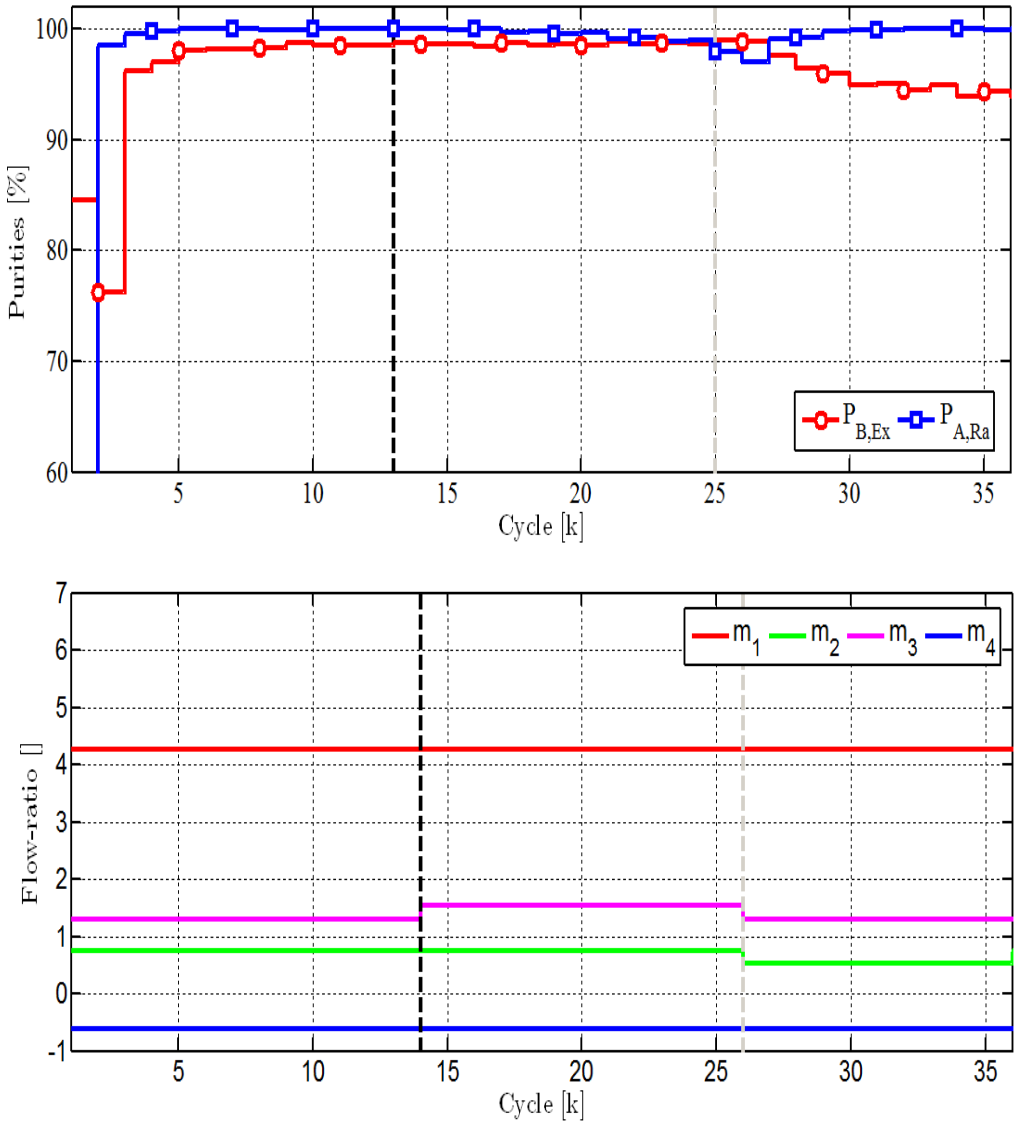

Figure 7: Third experimental validation of the parameter estimator. Disturbances of m_2 and m_3 at total separation.